Tuning the Casimir-Polder interaction via magneto-optical effects in graphene

T. Cysne, W. J. M. Kort-Kamp, D. Oliver, F. A. Pinheiro, F. S. S. Rosa, and C. Farina
Instituto de Física, Universidade Federal do Rio de Janeiro, Caixa Postal 68528, Rio de Janeiro 21941-972, RJ, Brazil
(Received 29 August 2014; published 17 November 2014)

We investigate the dispersive Casimir–Polder interaction between a rubidium atom and a suspended graphene sheet subjected to an external magnetic field **B**. We demonstrate that this concrete physical system allows for an unprecedented control of dispersive interactions at micro- and nanoscales. Indeed, we show that the application of an external magnetic field can induce an 80% reduction in the Casimir–Polder energy relative to its value without the field. We also show that sharp discontinuities emerge in the Casimir–Polder interaction energy for certain values of the applied magnetic field at low temperatures. Moreover, for sufficiently large distances, these discontinuities show up as a plateau-like pattern with a quantized Casimir–Polder interaction energy, in a phenomenon that can be explained in terms of the quantum Hall effect. In addition, we point out the importance of thermal effects in the Casimir–Polder interaction, which we show must be taken into account even for considerably short distances. In this case, the discontinuities in the atom-graphene dispersive interaction do not occur, which by no means prevents the tuning of the interaction in ∼50% by the application of the external magnetic field.

DOI: 10.1103/PhysRevA.90.052511 PACS number(s): 31.30.jh, 34.35.+a, 12.20.−m, 78.20.Ls

It has been known for a long time that quantum fluctuations give rise to interactions between neutral but polarizable objects (atoms, molecules, or even macroscopic bodies) which do not possess any permanent electric or magnetic multipoles. These are referred to as dispersive interactions, first explained in the nonretarded regime by Eisenchitz and London [1]. Retardation effects were first reported by Casimir and Polder [2,3] in works that pioneered the study of dispersive interactions between an atom and a perfectly conducting plane for arbitrary distances, generalizing the Lennard–Jones nonretarded result [4]. Since then these interactions, nowadays known as Casimir–Polder forces, have been diligently investigated both theoretically [5–11] and experimentally [12–18]. If instead of perfectly conducting plates one considers dispersive media, the calculations become more involved; this has motivated the development of a general theory of dispersive forces, including thermal effects [19,20]. Dispersive forces play an important role in many different areas of research and applications, ranging from biology and chemistry [21,22] to physics, engineering, and nanotechnology [8–10,23,24].

Recently, great attention has been devoted to dispersive interactions in carbon nanostructures, such as graphene sheets. These systems are especially appealing since graphene possesses unique mechanical, electrical, and optical properties [25]. Recently, dispersive interactions between graphene sheets and/or material planes have been investigated [26–39], as well as the Casimir–Polder interaction between atoms and graphene [40–45]. In particular, the impact of a graphene coating on the atom-plate interaction has been calculated for different atomic species and substrates; in some cases this results in modifications of the order of 20% in the strength of the interaction [44]. Furthermore, results on the possibility of shielding the dispersive interaction with the aid of graphene sheets have been reported [45].

However, the possibility of controlling the Casimir–Polder interaction between an atom and a graphene sheet by an external agent has never been envisaged so far. The possibility of varying the atom-graphene interaction without changing the physical system would be extremely appealing for both experiments and applications. With this motivation, and exploring the extraordinary magneto-optical response of graphene, in the present work we investigate the Casimir–Polder interaction between a rubidium atom and a suspended graphene sheet under the influence of an external magnetic field **B**. We show that, just by changing the applied magnetic field, the atom-graphene interaction can be greatly reduced by up to 80% of its value without the field. Furthermore, we demonstrate that, at low temperatures ($T \simeq 4$ K), the Casimir–Polder energy exhibits sharp discontinuities at certain values of B, which we show to be a manifestation of the quantum Hall effect. As the distance z between the atom and the graphene sheet grows to $z \gtrsim 1$ μm, these discontinuities form a plateau-like pattern with quantized values for the Casimir–Polder energy. We also show that, at room temperature ($T \simeq 300$ K), thermal effects must be taken into account even for considerably short distances. Moreover, in this case the discontinuities in the atom-graphene interaction do not occur, although the Casimir–Polder energy can still be tuned in ∼50% by applying an external magnetic field.

Let us consider that an isotropic particle is placed a distance z above a suspended graphene sheet biased by a static magnetic field $\mathbf{B} = B\hat{\mathbf{z}}$, as depicted in Fig. 1. The whole system is assumed to be in thermal equilibrium at temperature T. When $B \neq 0$ the optical properties of graphene can be well described in terms of a homogeneous but anisotropic two-dimensional conductivity tensor. In this case, the Casimir–Polder (CP) energy interaction can be calculated through the scattering approach and can be cast as [46]

$$U_T(z) = \frac{k_B T}{\varepsilon_0 c^2} {\sum_{l=0}^{\infty}}' \xi_l^2 \alpha(i\xi_l) \int \frac{d^2\mathbf{k}}{(2\pi)^2} \frac{e^{-2\kappa_l z}}{2\kappa_l} \times \left[r^{s,s}(\mathbf{k}, i\xi_l, B) - \left(1 + \frac{2c^2k^2}{\xi_l^2}\right) r^{p,p}(\mathbf{k}, i\xi_l, B) \right], \quad (1)$$

where $\xi_l = 2\pi l k_B T/\hbar$ are the so-called Matsubara frequencies, $\kappa_l = \sqrt{\xi_l^2/c^2 + k^2}$, $\alpha(i\xi)$ is the electric polarizability of the particle, and $r^{s,s}(\mathbf{k}, i\xi, B)$, $r^{p,p}(\mathbf{k}, i\xi, B)$ are the diagonal reflection coefficients associated with graphene. As usual, the

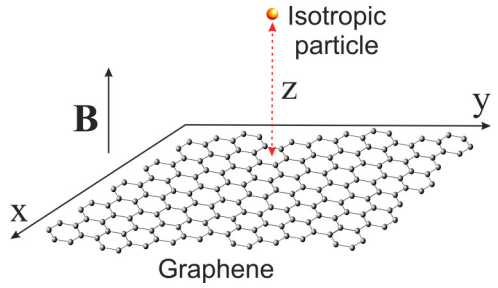

FIG. 1. (Color online) System of suspended graphene and an isotropic particle at a distance z, in presence of a static perpendicular magnetic field.

prime in the summation means that the zeroth term has to be weighted by a factor of $\frac{1}{2}$. Note that the cross-polarization reflection coefficients $r^{s,p}(\mathbf{k},i\xi,B)$ and $r^{p,s}(\mathbf{k},i\xi,B)$, despite being nonvanishing, do not appear in Eq. (1). This, however, does not mean that anisotropy plays no role in the interaction energy, as transverse conductivities or permittivities could still appear in $r^{s,s}(\mathbf{k},i\xi,B)$ and $r^{p,p}(\mathbf{k},i\xi,B)$. In particular, by modeling graphene as a two-dimensional (2-D) material with a surface density current $\mathbf{K}=\sigma\cdot\mathbf{E}|_{z=0}$ and applying the appropriate boundary conditions to the electromagnetic field, one can show that the reflection coefficients are [34]

$$r^{s,s}(\mathbf{k},i\xi,B)=\frac{2\sigma_{xx}(i\xi,B)Z^h+\eta_0^2[\sigma_{xx}(i\xi,B)^2+\sigma_{xy}(i\xi,B)^2]}{-\Delta(\mathbf{k},i\xi,B)}, \tag{2}$$

$$r^{p,p}(\mathbf{k},i\xi,B)=\frac{2\sigma_{xx}(i\xi,B)Z^e+\eta_0^2[\sigma_{xx}(i\xi,B)^2+\sigma_{xy}(i\xi,B)^2]}{\Delta(\mathbf{k},i\xi,B)}, \tag{3}$$

$$\Delta(\mathbf{k},i\xi,B)=[2+Z^h\sigma_{xx}(i\xi,B][2+Z^e\sigma_{xx}(i\xi,B)]+[\eta_0\sigma_{xy}(i\xi,B)]^2, \tag{4}$$

where $Z^h=\xi\mu_0/\kappa$, $Z^e=\kappa/(\xi\epsilon_0)$, and $\eta_0^2=\mu_0/\epsilon_0$. Besides, $\sigma_{xx}(i\xi,B)$ and $\sigma_{xy}(i\xi,B)$ are the longitudinal and transverse conductivities of graphene, respectively.

The electric conductivity tensor of graphene under an external magnetic field is well known and reads [47,48]

$$\sigma_{xx}(i\xi,B)=\frac{e^3v_F^2B\hbar(\xi+\tau^{-1})}{\pi}\sum_{n=0}^{\infty}\left\{\frac{n_F(M_n)-n_F(M_{n+1})+n_F(-M_{n+1})-n_F(-M_n)}{D_n(M_{n+1}-M_n)}+(M_n\to-M_n)\right\}, \tag{5}$$

$$\sigma_{xy}(i\xi,B)=\frac{e^3v_F^2B}{-\pi}\sum_{n=0}^{\infty}\{n_F(M_n)-n_F(M_{n+1})-n_F(-M_{n+1})+n_F(-M_n)\}\left[\frac{1}{D_n}+(M_n\to-M_n)\right], \tag{6}$$

where $1/\tau$ is a phenomenological scattering rate, $n_F(E)$ is the Fermi–Dirac distribution, $D_n=(M_{n+1}-M_n)^2+\hbar^2(\xi+\tau^{-1})^2$, and $M_n=\sqrt{n}M_1$ are the Landau energy levels, $M_1^2=2\hbar eBv_F^2$ is the Landau energy scale, and $v_F\simeq10^6$ m/s is the Fermi velocity. Also, in the following we use $\tau=1.84\times10^{-13}$ s and set the chemical potential to be $\mu_c=0.115$ eV.

We still have to specify the particle in our setup. It turns out that a rubidium atom is a convenient choice, since there are experimental data on its complex electric polarizability $\alpha(\omega)$ for a wide range of frequencies [49]. At this point it is worth mentioning that the rubidium ground-state polarizability is strongly dominated by the D-line transitions [50], which occur around 380 THz. Even though Zeeman shifts $\sim$0.05 THz/T (strong-magnetic-field regime) do exist at these transitions [51], we checked that they are negligible for calculations of the dispersive interaction for the values of B used throughout the paper. Finally, as is clear from Eq. (1), we actually need the polarizability evaluated at imaginary frequencies, which can be readily be obtained from the Kramers–Kronig relations provided one has the data for $\mathrm{Im}\alpha(\omega)$ [46].

Our first results are summarized in Fig. 2(a), where we depict the CP energy of our setup as a function of the atom-graphene distance z and magnetic field B for $T=4$ K (normalized by its corresponding value for $B=0$ T). The hallmark of this plot is, surely, the great amount of discontinuities shown by the energy as a function of B for all distances considered. These drops show up even more clearly in Figs. 2(b) and 2(c), where we take two cuts of Fig. 2(a) at two different fixed values of z; namely, $z=100$ nm and $z=1$ μm, and present them as 2-D plots. Such discontinuities are directly linked to the discrete Landau levels brought about by the application of a magnetic field. In order to understand the situation, let us consider the energy-momentum dispersion diagram of graphene in the presence of a static magnetic field depicted in Fig. 3. On the left the usual linear dispersion relation of graphene is presented by the blue solid line. Due to the magnetic field the carriers in graphene can occupy only the discrete values of energy given by the Landau levels M_n represented by black dots. The allowed transitions between two Landau levels give rise to all terms of the summations in Eqs. (6) and (7). There are two kinds of transitions: interband transitions, which connect levels at distinct bands (e.g., long arrow between $-M_{n_c}$ and M_{n_c+1}), and intraband transitions that involve levels at the same band (e.g., short arrow between M_{n_c} and M_{n_c+1}). The possibility of a specific transition occurring is related to the difference between the probabilities of having the initial and final levels full and empty, respectively. Ultimately, these probabilities are given by the Fermi–Dirac distribution (solid orange line on the right of Fig. 3). Hence, whenever a given Landau level, whose position in energy depends on B, crosses upwards (downwards) the chemical potential (dot-dashed green line) of the graphene sheet, it gets immediately depopulated (populated) as a consequence of the quasi-step-function character of the Fermi–Dirac distribution

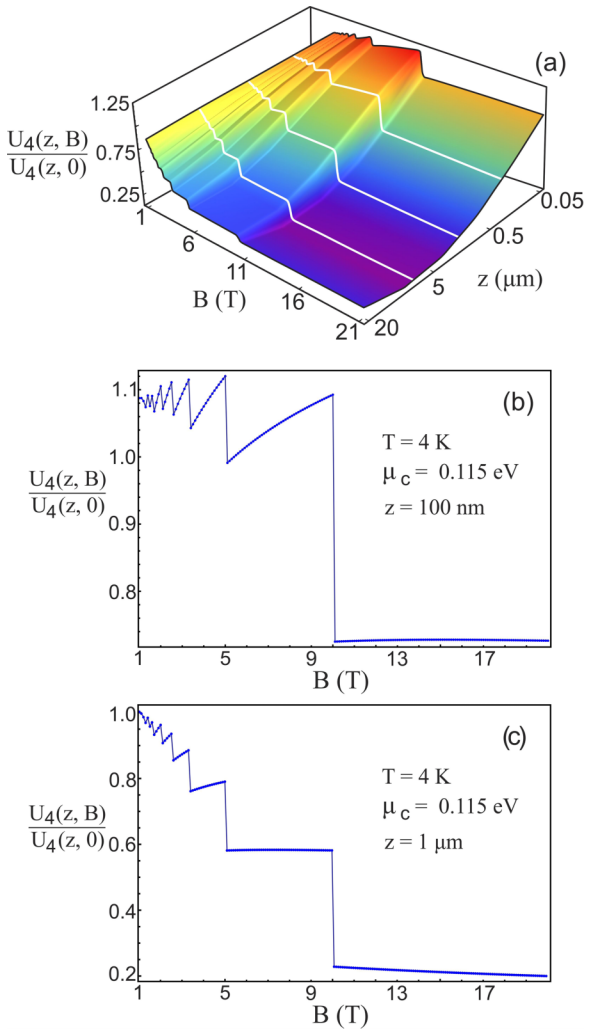

FIG. 2. (Color online) (a) The Casimir–Polder energy of a rubidium atom in front of a graphene sheet subjected to a magnetic field B as a function of B and distance z. (b), (c) The Casimir–Polder energy as a function of B for two fixed distances: (b) $z = 100$ nm, and (c) $z = 1$ μm. In all plots $\mu_c = 0.115$ eV, $T = 4$ K, and we have normalized $U_4(z,B)$ by the energy in the absence of magnetic field, $U_4(z,0)$.

at 4 K. Therefore, the crossing of the nth level sharply quenches the $M_n \leftrightarrow M_{n+1}$ transition; at the same time it gives birth to the $M_{n-1} \leftrightarrow M_n$ transition [47,48] in a process that discontinuously changes the conductivity and thus the interaction energy. The fact that the CP energy always drops *down* at a discontinuity as we increase B may be understood by recalling the behavior of the relativistic Landau levels with $\sqrt{n}$ (see above). This square-root growth implies that the $n-1 \leftrightarrow n$ gap is wider than the $n \leftrightarrow n+1$ gap, making the transition weaker and hence reducing the overall conductivity. A similar analysis is valid for the interband transitions.

Figure 2 also reveals that a flattening of the steps in the CP energy between drops occurs as B increases. However, if on the one hand for $z = 100$ nm only the very last step is really flat, on the other hand many plateau-like steps exist for $z = 1$ μm. This result is connected to the electrostatic limit of the conductivity: for large distances the exponential

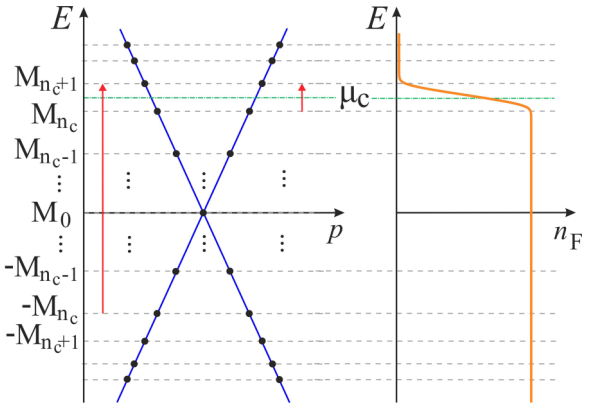

FIG. 3. (Color online) The left side shows the energy-momentum dispersion diagram of graphene in a magnetic field. The blue lines show the usual linear dispersion relation of graphene while the Landau levels brought forth by the introduction of B are represented by the black dots. The long (short) vertical arrow shows the lowest energy interband (intraband) transition crossing the chemical potential (dot-dashed green line). The right side shows the Fermi–Dirac distribution at temperature T.

factor in Eq. (1) strongly suppress all contributions coming from $l \neq 0$, whereas for $l = 0$ and large magnetic fields $\sigma_{xx} \sim 0$ and $\sigma_{xy} \sim \pm(2N+1)e^2/(\pi\hbar)$, where N is an integer [25]. Therefore, in the limit of large distances (of the order of micrometers) only the Hall conductivity contributes to $U_4(z,B)$, and the CP energy became almost quantized [34]. Furthermore, one should note the striking reduction in the force as we sweep through different values of B. While for $z = 100$ nm this reduction can be as hight as 30%, one can get up to an impressive 80% decrease in the CP interaction for $z = 1$ μm and $B \gtrsim 10$ T, with huge drops in between. Finally, it should be remarked that, for $B \gtrsim 10$ T, the CP interaction is practically insensitive to changes in the magnetic field, regardless of the atom-graphene distance. In this regime the discontinuities in the CP energy do not occur any longer. This effect has its origins in the fact that there is a critical value of the magnetic field B_c (in the present case, $B_c \sim 10$ T) for which the transition $M_0 \rightarrow M_1$ is dominant since all Landau levels, except M_0, are above the chemical potential. The value of the critical magnetic field can be estimated by solving the equation $\mu_c = M_1 = \sqrt{2\hbar e B_c v_F^2}$. Altogether, our findings suggest that the atom-graphene system is particularly suited for investigation of the effects of external magnetic fields on CP forces and may pave the way for an active modulation of dispersion forces in general.

In order to investigate thermal effects, in Fig. 4(a) we present the CP energy as a function of both z and B at room temperature. The most distinctive aspect of Fig. 4(a) is the complete absence of discontinuities that characterize the behavior of the CP energy at low temperatures. At $T = 300$ K the Fermi–Dirac distribution is a quite smooth function of the energy levels, allowing for a partial filling of many Landau levels. Hence the effects of the crossing between these levels and the graphene's chemical potential is hardly noticed, resulting in a smooth CP energy profile. Indeed, we checked that, even for temperatures of a few dozen kelvin, the

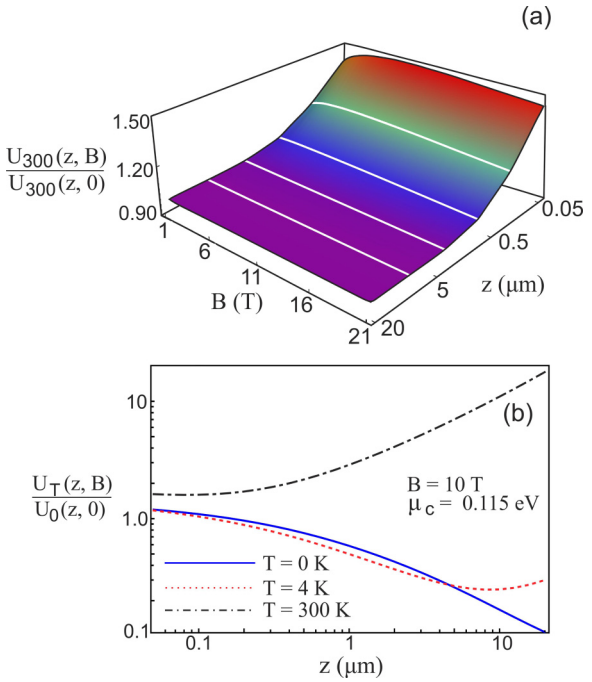

FIG. 4. (Color online) (a) The Casimir–Polder interaction energy $U_{300}(z,B)$ [normalized by $U_{300}(z,0)$] between a rubidium atom and a graphene sheet as a function of both distance and external magnetic-field strength for $T = 300$ K. (b) The Casimir–Polder energy [normalized by $U_0(z,0)$] as a function of the mutual distance between atom and graphene sheet for $T = 0$ K (solid line), $T = 4$ K (dashed line), and $T = 300$ K (dot-dashed line). In both panels (a) and (b) the graphene chemical potential is $\mu_c = 0.115$ eV.

discontinuities in the interaction are not present any longer. Another important aspect of Fig. 4(a) is that the CP energy becomes essentially independent of B for $z \gtrsim 1$ μm. For this set of parameters, the system is already in the thermal regime, where the CP energy is essentially dominated by the electrostatic conductivity. In this regime, the CP energy is very weakly affected by variations in B due the already-discussed exponential suppression of the $l \geqslant 1$ terms in Eq. (1). We emphasize, however, that the absence of discontinuities does not prevent one from tuning the CP interaction between a Rb atom and a graphene sheet, at least at short distances. This tunability can be achieved even for relatively modest magnetic fields, as the value of the CP energy can increase up to 50% (compared to the case where $B = 0$ T) by applying a magnetic field of $B = 5$ T for $z = 50$ nm. For $B = 5$ T and $z = 100$ nm, the variation in the interaction can still be as high as 30%. In Fig. 4(b) the CP energy is calculated for $B = 10$ T and for different temperatures: $T = 0$, 4, and 300 K, all normalized by the zero-temperature, zero-field energy value $U_0(z,0)$. Figure 4(b) reveals that thermal corrections are relevant even for low temperatures, and for a broad range of distances: we have a 10%–20% variation in the relative difference of $U_4(z,10)$ and $U_0(z,10)$ in the 1–10 μm interval, which is in the ballpark of the precision of recent and current experiments. Besides, Fig. 4(b) demonstrates that, at room temperature, not only the thermal effects are absolutely dominant in the micrometer range, but they also play an important role even for small distances. Indeed, at $z = 100$ nm the relative difference between $U_{300}(z,10)$ and $U_0(z,10)$ is $\sim$45% and at $z = 1$ μm it is $\sim$400%; so in the latter approximately 80% of the CP energy comes from the thermal contribution. We conclude that, at room temperature, these effects should be taken into account for a wide range of distances between the atom and the graphene sheet.

In conclusion, we investigated the dispersive Casimir–Polder interaction between a rubidium atom and a suspended graphene sheet subjected to an external magnetic field **B**. Apart from providing a concrete physical system where the dispersive interaction in nano- and micrometer scales can be controlled by an external agent, we show that, just by changing the applied magnetic field, this interaction can be reduced by up to 80% of its value in the absence of the field. Furthermore, due to the quantum Hall effect, we show that, for low temperatures, the Casimir–Polder interaction energy acquires sharp discontinuities at given values of B and that these discontinuities approach a plateau-like pattern with a quantized Casimir–Polder interaction energy as the atom and the graphene sheet become farther and farther apart. In addition, we show that, at room temperature, thermal effects must be taken into account even for considerably short distances. In this case, the discontinuities in the atom-graphene dispersive interaction are not present any longer, although the interaction can still be tuned in $\sim$50% by applying an external magnetic field.

We thank P. A. Maia Neto for assistance with the rubidium data, and R. S. Decca, I. V. Fialkovsky, E. C. Marino, and N. M. R. Peres for useful discussions. We also acknowledge CNPq and FAPERJ for partial financial support. T.C. and W.J.M.K.-K. contributed equally to this work.

[1] R. Eisenschitz and F. London, Z. Phys. **60**, 491 (1930); F. London, *ibid.* **63**, 245 (1930).
[2] H. B. G. Casimir and D. Polder, Nature (London) **158**, 787 (1946).
[3] H. B. G. Casimir and D. Polder, Phys. Rev. **73**, 360 (1948).
[4] J. E. Lennard-Jones, Trans. Faraday Soc. **28**, 333359 (1932).
[5] S. Y. Buhmann and D.-G. Welsch, Prog. Quantum Electron. **31**, 51 (2007).
[6] S. Y. Buhmann, *Dispersion Forces I. Macroscopic Quantum Electrodynamics and Ground-State Casimir, Casimir–Polder and van der Waals Forces* (Springer, Heidelberg, 2013); *Dispersion Forces II - Many-Body Effects, Excited Atoms, Finite Temperature and Quantum Friction* (Springer, Heidelberg, 2013).
[7] P. W. Milonni, *The Quantum Vacuum: An Introduction to Electrodynamics* (Academic Press, San Diego, 1994).
[8] *Casimir Physics*, Lecture Notes in Physics Vol. 834, edited by D. Dalvit, P. Milonni, D. Roberts, and F. S. S. Rosa (Springer, Heidelberg, 2010).
[9] G. L. Klimchitskaya, U. Mohideen, and V. M. Mostepanenko, Rev. Mod. Phys. **81**, 1827 (2009).
[10] M. Bordag, G. L. Klimchitskaya, U. Mohideen, and V. M. Mostepanenko, *Advances in the Casimir Effect* (Oxford University Press, Oxford, 2009).

[11] D. P. Craig and T. Thirunamachandran, *Molecular Quantum Electrodynamics* (Dover, New York, 1998).
[12] V. Druzhinina and M. DeKieviet, Phys. Rev. Lett. **91**, 193202 (2003).
[13] A. Laliotis, T. P. de Silans, I. Maurin, M. Ducloy, and D. Bloch, Nat. Commun. **5**, 4364 (2014).
[14] J. M. Obrecht, R. J. Wild, M. Antezza, L. P. Pitaevskii, S. Stringari, and E. A. Cornell, Phys. Rev. Lett. **98**, 063201 (2007).
[15] T. A. Pasquini, Y. Shin, C. Sanner, M. Saba, A. Schirotzek, D. E. Pritchard, and W. Ketterle, Phys. Rev. Lett. **93**, 223201 (2004).
[16] F. Shimizu, Phys. Rev. Lett. **86**, 987 (2001).
[17] C. I. Sukenik, M. G. Boshier, D. Cho, V. Sandoghdar, and E. A. Hinds, Phys. Rev. Lett. **70**, 560 (1993).
[18] A. Landragin, J.-Y. Courtois, G. Labeyrie, N. Vansteenkiste, C. I. Westbrook, and A. Aspect, Phys. Rev. Lett. **77**, 1464 (1996).
[19] E. M. Lifshitz, Zh. Eksp. Teor. Fiz. **29**, 94 (1955) [Sov. Phys. JETP **2**, 73 (1956)].
[20] I. E. Dzyaloshinskii and L. P. Pitaevskii, Sov. Phys. JETP **9**, 1282 (1959); I. E. Dzyaloshinskii, E. M. Lifshitz, and L. P. Pitaevskii, Adv. Phys. **10**, 165 (1961).
[21] K. Autumn, M. Sitti, Y. A. Liang, A. M. Peattle, W. R. Hansen, S. Sponberg, T. W. Kenny, R. Fearing, J. N. Israelachvili, and R. J. Full, Proc. Natl. Acad. Sci. USA **99**, 12252 (2002).
[22] J. Klimes and A. Michaelides, J. Chem. Phys. **137**, 120901 (2012).
[23] K. A. Milton, J. Phys. A: Math. Gen. **37**, R209 (2004).
[24] S. K. Lamoreaux, Rep. Prog. Phys. **68**, 201 (2005).
[25] A. B. C. Neto, F. Guinea, N. M. R. Peres, K. S. Novoselov, and A. K. Geim, Rev. Mod. Phys. **81**, 109 (2009); N. M. R. Peres, *ibid.* **82**, 2673 (2010).
[26] M. Bordag, I. V. Fialkovsky, D. M. Gitman, and D. V. Vassilevich, Phys. Rev. B **80**, 245406 (2009).
[27] G. Gómez-Santos, Phys. Rev. B **80**, 245424 (2009).
[28] D. Drosdoff and L. M. Woods, Phys. Rev. B **82**, 155459 (2010).
[29] V. Svetovoy, Z. Moktadir, M. Elwenspoek, and H. Mizuta, Europhys. Lett. **96**, 14006 (2011).
[30] I. V. Fialkovsky, V. N. Marachevsky, and D. V. Vassilevich, Phys. Rev. B **84**, 035446 (2011).
[31] D. Drosdoff and L. M. Woods, Phys. Rev. A **84**, 062501 (2011).
[32] B. E. Sernelius, Phys. Rev. B **85**, 195427 (2012).
[33] M. Bordag, G. L. Klimchitskaya, and V. M. Mostepanenko, Phys. Rev. B **86**, 165429 (2012).
[34] W.-K. Tse and A. H. MacDonald, Phys. Rev. Lett. **109**, 236806 (2012).
[35] A. D. Phan, L. M. Woods, D. Drosdoff, I. V. Bondarev, and N. A. Viet, Appl. Phys. Lett. **101**, 113118 (2012).
[36] G. L. Klimchitskaya and V. M. Mostepanenko, Phys. Rev. B **87**, 075439 (2013).
[37] D. Drosdoff, A. D. Phan, L. M. Woods, I. V. Bondarev, and J. F. Dobson, Eur. Phys. J. B **85**, 365 (2012).
[38] A. D. Phan, T. X. Hoang, T.-L. Phan, and L. M. Woods, J. Chem. Phys. **139**, 184703 (2013).
[39] G. L. Klimchitskaya and V. M. Mostepanenko, Phys. Rev. B **89**, 035407 (2014).
[40] Yu. V. Churkin, A. B. Fedortsov, G. L. Klimchitskaya, and V. A. Yurova, Phys. Rev. B **82**, 165433 (2010).
[41] T. E. Judd, R. G. Scott, A. M. Martin, B. Kaczmarek, and T. M. Frohold, New J. Phys. **13**, 083020 (2011).
[42] M. Chaichian, G. L. Klimchitskaya, V. M. Mostepanenko, and A. Tureanu, Phys. Rev. A **86**, 012515 (2012).
[43] C. Eberlein and R. Zietal, Phys. Rev. A **86**, 062507 (2012).
[44] G. L. Klimchitskaya and V. M. Mostepanenko, Phys. Rev. A **89**, 062508 (2014).
[45] S. Ribeiro and S. Scheel, Phys. Rev. A **88**, 042519 (2013); **89**, 039904(E) (2014).
[46] A. M. Contreras-Reyes, R. Guérout, P. A. Maia Neto, D. A. R. Dalvit, A. Lambrecht, and S. Reynaud, Phys. Rev. A **82**, 052517 (2010).
[47] V. P. Gusynin and S. G. Sharapov, Phys. Rev. B **73**, 245411 (2006).
[48] V. P. Gusynin, S. G. Sharapov, and P. Cabotte, J. Phys.: Condens. Matter **19**, 026222 (2007).
[49] A. Derevianko, S. G. Porsev, and J. F. Babb, At. Data Nucl. Data Tables **96**, 323 (2010).
[50] J. Mitroy, M. S. Safronova, and Charles W. Clark, J. Phys. B: At. Mol. Opt. Phys. **43**, 202001 (2010).
[51] D. A. Steck, Rubidium 85 *D*-Line Data, available online at http://steck.us/alkalidata (2013).